Dry Sliding Wear Behavior of Hot-Dip Aluminized Ti-6Al-4V Alloy as a Function of Sliding Velocity

Wei Jiang, Benguo Zhang, Wei Chen, Shuqi Wang, and Xianghong Cui

An aluminized coating was prepared on Ti-6Al-4V alloy by hot-dip aluminizing and subsequently diffusion treatment. Dry sliding wear tests were performed for the aluminized and uncoated Ti-6Al-4V alloy under the loads of 10-50 N at the sliding velocities of 0.5-4 m/s. The wear resistance of the titanium alloy was improved by the aluminized coating under various conditions, especially at 4 m/s. The improved wear performance was suggested to be attributed to the Ti-Al coating and tribo-oxide layer. Tribo-layers were identified to form on worn surfaces under various conditions but their influence on the wear behavior and mechanism was decided by the amount and kind of oxides. The outmost values of the microhardness distribution at subsurfaces as a function of load could be used to identify the property and stability of tribo-layers. At 4 m/s, oxide-containing tribo-layers (more TiO, TiO_2 and trace Fe_2O_3) presented high hardness and stability, thus possessed an obvious wear-reduced function. Conversely at 2.68 m/s, no-oxide tribo-layers did not show the protection from wear because of their lower hardness and instability. The formation of tribo-layers under various sliding speeds was noticed to be a process including wear debris production, oxidation and accumulation and densification, even sintering.

1. Introduction

Titanium alloys are widely used in aerospace, seawater desalination, automobile and other fields because of high specific strength, low density and excellent corrosion resistance (Ref 1-3). However, it is well known that titanium alloys possess poor tribological performance. This was attributed to their low resistance to plastic shearing, low work hardening and especially non-protective tribo-oxides (Ref 4-12). Such a poor tribological performance obviously limits the application of titanium alloys in many areas including sliding. Therefore, various surface treatment routes are usually applied to improve their tribological performance. For example, microarc oxidation plasma nitridation, laser cladding, thermal oxidation and physical vapor deposition were used to improve the wear resistance of titanium alloys, as reported by the literature (Ref 6, 13-17). It is clear that hot-dip aluminizing is a competitive method due to its low cost, simple operation and thick coating. Compared with titanium alloys, titanium aluminides present lower density, higher elastic modulus, higher oxidation resistance and better mechanical behavior with temperature (Ref 18-21). Therefore, titanium aluminides have aroused great interest in high-temperature applications because of their ordered structure and the strong covalent bonding between atoms

(Ref 18). However, the low ductility at room temperature prevents Ti_3Al, TiAl and $TiAl_3$ from being widely applied as structural materials (Ref 18,22). Alternatively, the titanium aluminides can be directly used as coatings and presented a promising and effective application (Ref 23,24). If aluminized coatings possess higher wear performance than titanium alloys, the application scope of titanium alloys would be enlarged. However, the research on the wear behavior of aluminized titanium alloys as a function velocity was sparsely reported.

The present research was designed to explore the wear behavior and mechanism of the aluminized coating. A hot-dip aluminizing and subsequently a diffusion annealing treatment at 650 °C was used to produce the aluminized coating of $TiAl_3$ on Ti-6V-4V alloy. Dry sliding wear tests for an aluminized Ti-6Al-4V alloy against AISI 52100 steel were performed at room temperature and 0.5-4 m/s. The morphology, composition, phase and property of worn surfaces and subsurfaces were investigated by scanning electron microscopy (SEM), energy-dispersive spectroscopy (EDS), x-ray diffractometer (XRD), x-ray photoelectron spectroscopy (XPS) and microhardness tester, respectively.

2. Experimental Procedure

A commercial Ti-6Al-4V alloy (wt.%) (Ti-6.3Al-4.0V) as the substrate material, was machined into a pie-shaped specimen with a dimension of Φ30 mm × 23 mm. The surface of the specimen was polished (Ra. 0.38 μm), cleaned by ultrasonically washing in acetone and dried in air. Then, the pretreated Ti-6Al-4V alloy was immersed into a melting bath of high pure aluminum (Al ≥ 99.99 wt.%) for 15 min at 760 °C, subsequently taken out at a modest speed and finally cooled in air. Then, a diffusion annealing treatment was performed for the encased Ti-6Al-4V alloy at 650 °C for 0.5 h to achieve an aluminized coating.

Wei Jiang, Wei Chen, Shuqi Wang, and **Xianghong Cui**, School of Materials Science and Engineering, Jiangsu University, Zhenjiang 212013, China; **Benguo Zhang**, School of Materials Science and Engineering, Jiangsu University, Zhenjiang 212013, China; and School of Mechanical Engineering, Yancheng Institute of Technology, Yancheng 224002, China. Contact e-mails: shuqi_wang@ujs.edu.cn715714561@qq.com.

Dry sliding wear tests were performed in air on an MPX-2000 type pin-on-disk wear tester. The aluminized and uncoated Ti-6Al-4V alloys were machined into pins with the dimensions of 5 mm in diameter and 23 mm in height. Commercial AISI 52100 steel (wt.%) (Fe-1.02C-1.55Cr), as the mating material, was austenitized at 850 °C, oil quenched, and finally tempered at 400 °C for 2 h to achieve a hardness of 50 HRC. The parameters of wear tests were selected to be 0.5, 0.75, 1.5, 2.68 and 4 m/s for the sliding velocity; 10-50 N with an interval of 20 N for the normal load; room temperature at 23-28 °C for the experimental temperature; 840 m for the sliding distance. The mass loss of pins before and after tests was measured as the wear losses by an electronic balance with an accuracy of 0.01 mg. Three repeated tests were needed to achieve the mean value as the experimental result. A JSM-7001F scanning electron microscopy (SEM), an Inca Energy 350 energy-dispersive spectroscopy (EDS), and a D/Max-2500/pc x-ray diffractometer (XRD) were used to investigate the morphologies, compositions and phases of the aluminized coating and worn surfaces, respectively. A Kratos Axis Ultra DLD x-ray photoelectron spectroscopy (XPS) was applied to further identify trace oxides on worn surfaces. The microhardness of the aluminized coating and worn subsurface was determined by an HVS-1000 digital microhardness tester with a load of 0.49 N and a hold time of 15 s. The hardness of the steels after heat treatment was measured by an HR-150A Rockwell apparatus.

3. Result and Analysis

3.1 Microstructure of Aluminized Ti-6Al-4V Alloy

Figure 1 illustrates the microstructural characteristics of the aluminized Ti-6Al-4V alloy. As shown in the XRD pattern, $TiAl_3$ was identified to be the main phase of the aluminized coating. The cross-sectional morphology of the aluminized coating is shown in Fig. 1(b). The intermetallic coating presented a fine microstructure and a flat, smooth interface with the substrate. The regional semi-quantitative analysis EDS_1 (Fig. 1c) indicates that the atomic ratio of this aluminized coating was approximate to the stoichiometric ratio of $TiAl_3$. The formation of $TiAl_3$ coating could be attributed to the fact that Ti and Al atoms moved outward and inward through the elevated-temperature diffusion at 650 °C. $TiAl_3$ coating presented the microhardness of 500-585 HV.
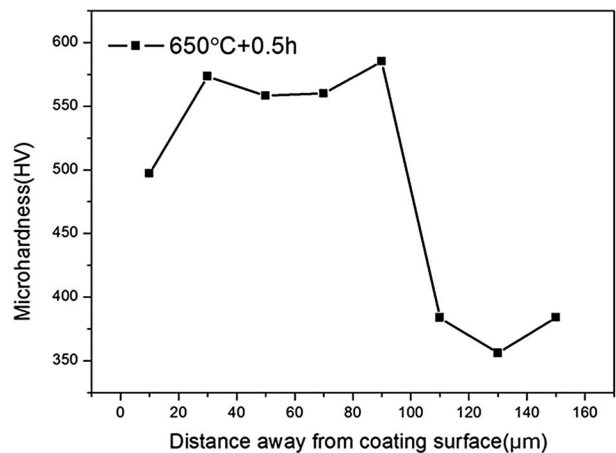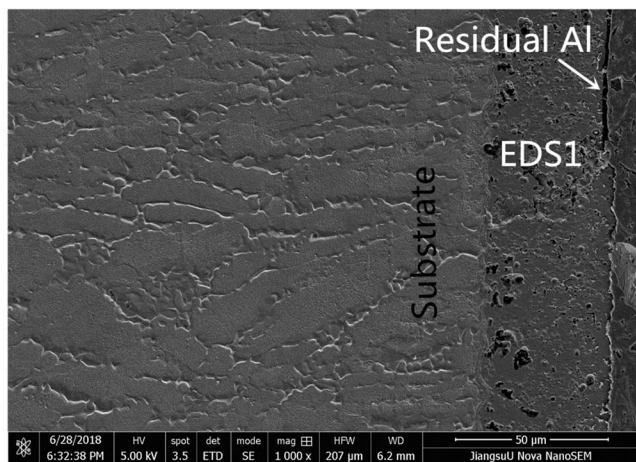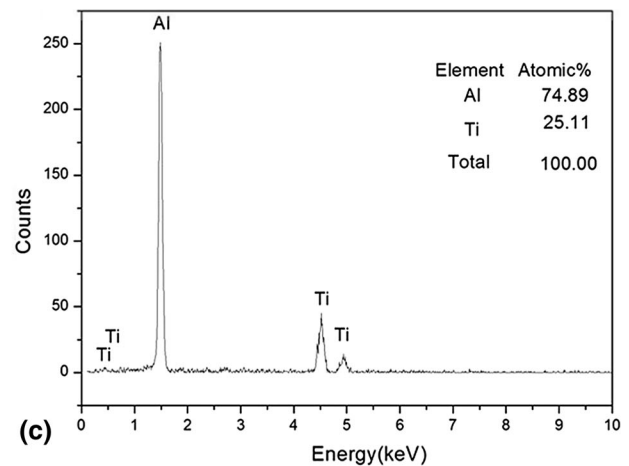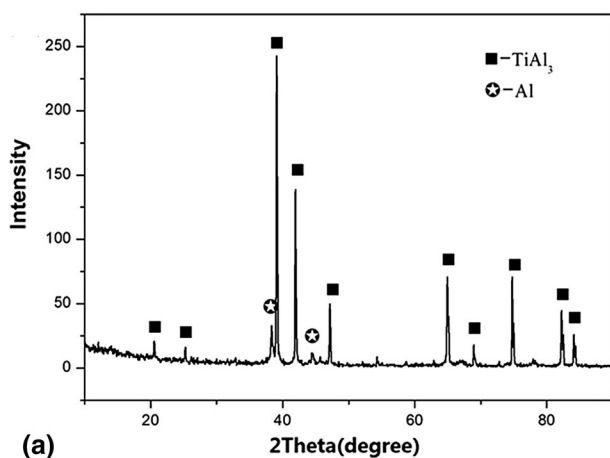
Fig. 1 Microstructural characteristics of the aluminized coating on Ti-6Al-4V alloy: XRD pattern (a), cross-sectional morphology (b), EDS analysis (c), microhardness distribution (d)

3.2 Wear Behavior of Aluminized and Uncoated Ti-6Al-4V Alloy

Figure 2(a) illustrates the wear loss *vs.* sliding velocity histogram of the aluminized Ti-6Al-4V alloy. The aluminized Ti-6Al-4V alloy presented an increased wear loss with the load under various velocities. In particular, a violent increase occurred at 2.68 m/s. Under various loads, almost the same variation trend of wear loss as a function of sliding velocity was presented. As shown in Fig. 2(a), the wear loss firstly decreased to a turning point at 0.75 m/s, and then rapidly increased to reach the climax at 2.68 m/s, and finally substantially decreased to the lowest point at 4 m/s. Here, the wear characteristics of the aluminized Ti-6Al-4V alloy at 0.75, 2.68 and 4 m/s were focused on to be explored.

Figure 2(b) presents the comparison of the wear loss between the aluminized and uncoated Ti-6Al-4V alloy. It is clear that the aluminized and uncoated Ti-6Al-4V alloy almost possessed the same variation regularity of wear loss with an increase in sliding velocity under various loads. Their wear behavior was similar to Li's research results on the sliding wear of Ti-6Al-4V alloy (Ref 25). Clearly, the aluminized Ti-6Al-4V possessed an absolutely lower wear loss than uncoated Ti-6Al-4V alloy at different sliding velocities, no matter whatever load

was applied. It can be suggested that the aluminized coating substantially improved the wear resistance of the Ti-6Al-4V alloy, especially at higher velocity and load. Thus, the aluminized coating could protect Ti-6Al-4V alloy from wear to some extent.

3.3 Morphology of Worn Surfaces

The morphology of worn surfaces for the aluminized Ti-6Al-4V alloy is illustrated in Fig. 3. A composite pattern containing adhesive and tribo-oxide vestiges were presented at 0.75 m/s, as shown in Fig. 3(a) and (b). However, tribo-oxide vestiges totally disappeared at 2.68 m/s. The worn surfaces revealed many furrows and more deep delamination places, which were resulted from the plowed marks and the delamination of matrix, as shown in Fig. 3(c) and (d). After sliding at 4 m/s, the aluminized coating presented totally different morphologies of the worn surfaces from those at 2.68 m/s. Compacted tribo-layers and less shallow delaminated regions were observed to appear on worn surfaces, as shown in Fig. 3(e) and (f). EDS results demonstrate that the oxygen content of the worn surface under 50 N was identified to be 27.68 wt.% (EDS_1) at 0.75 m/s, zero (EDS_2) at 2.68 m/s, and 50.33 wt.% (EDS_3) at 4 m/s, as shown in Fig. 4.

3.4 Identification of Tribo-Layers

The existence of tribo-layers is readily distinguished by cross-sectional morphology of worn subsurfaces. Figure 5 illustrates the cross-sectional morphology of worn subsurfaces of the aluminized Ti-6Al-4V alloy. Regardless of velocities, tribo-layers were noticed to always form on the worn surfaces. The tribo-layer was observed to be uncompacted with a thick plastic deformation region at 0.75 m/s. However, as the load increased to 50 N, the tribo-layer became more compact with a thinner plastic deformed layer (Fig. 5a and b). As shown in Fig. 5(c) and (d), there exist a discontinuous tribo-layer and a thicker plastic deformed layer at 2.68 m/s. Conversely, at 4 m/s, compact, continuous tribo-layers appeared and seemed to possess a higher load-bearing capability. Thus, the plastic deformation region became smaller, even disappeared under 50 N, as shown in Fig. 5(e) and (f).

Figure 6 illustrates the XRD patterns of worn surfaces for the aluminized Ti-6Al-4V alloy sliding under 10 and 50 N at 0.75, 2.68 and 4 m/s. The worn surface at 0.75 m/s presented Ti and TiO, but no $TiAl_3$ coating, as shown in Fig. 6(a). This meant that at 0.75 m/s, the $TiAl_3$ coating was totally peeled off after 840 m of sliding. In addition, the oxide amount seemed to increase slightly with an increase in load. When the sliding velocity reached 4 m/s, more TiO and TiO_2 appeared and the oxide amount increased with the increase in load. Meanwhile, $TiAl_3$ coating was noticed to exist on the worn surface at 50 N, as shown in Fig. 6(a). This meant that the $TiAl_3$ coating was partly peeled off after 840 m of sliding. This is because the coating or tribo-oxide layer became strong at 4 m/s. Conversely, at 2.68 m/s, merely trace TiO appeared under 10 N, especially no oxide remained under 50 N on the worn surfaces, as shown in Fig. 6(a). In addition, the $TiAl_3$ coating was totally peeled off after sliding because of no protection of tribo-layers.

It is clear that tribo-oxidation occurred during sliding. As shown in XRD patterns of worn surfaces, the formation or delamination (peeling off) of tribo-oxides under various sliding conditions could be deduced. The existence of tribo-oxides is well known to take effect on the wear behavior and mechanism
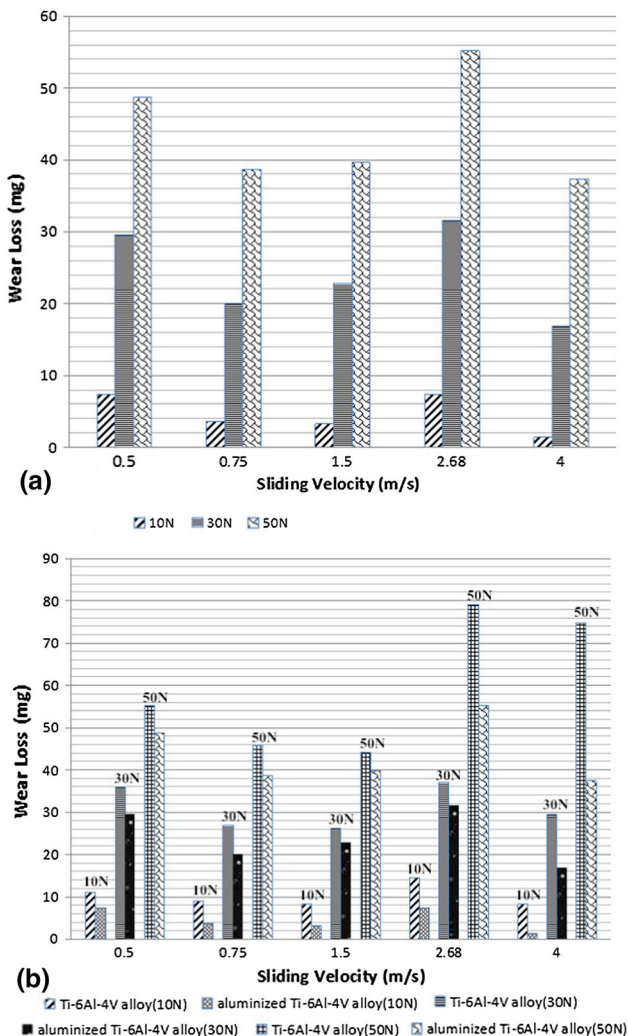

(a)

(b)

Fig. 2 Wear loss of aluminized and uncoated Ti-6Al-4V alloy as a function of sliding velocity under various loads

(Ref 11,25). More importantly, the amount of tribo-oxides as a function of load revealed the tendency of the stable existence or delamination of tribo-oxides. XPS was employed to identify trace oxides on worn surfaces. XPS spectra of Fe 2p on the worn surfaces at 50 N, and sliding speeds of 2.68 and 4 m/s are shown in Fig. 6(b). At 2.68 m/s, there was no XPS peak of Fe 2p on the worn surface. On the contrary, at 4 m/s, the XPS peaks of Fe 2p assigned to Fe_2O_3 were noticed. This indicates that Fe_2O_3 existed on worn surfaces, but did not at 2.68 m/s.

In order to evaluate the load-bearing capability of tribo-layers, the microhardness distribution of the cross-sectional worn surfaces of aluminized Ti-6Al-4V alloy was measured, as shown in Fig. 7. The worn surfaces and subsurfaces presented marked changes of microhardness, especially the outermost microhardness after sliding at various velocities. But the substrate maintained the original hardness ranging about 300-390 HV. Clearly, the microhardness of subsurfaces presented a ladder-shaped distribution. The hardness reached higher values at the outermost part, and then rapidly decreased to the original one of substrate. More importantly, different microhardness values appeared at the outermost position after sliding at various velocities, from which the load-bearing capability of tribo-layers could be estimated. Under 10 and 50 N, the outermost microhardness increased from 397 to 510 HV at 0.75 m/s, from 628 to 772 HV at 4 m/s, but decreased from 491 to 390 HV at 2.68 m/s. Clearly, the outermost microhardness came from the tribo-layers, thus roughly depending on their characteristics. More interestingly, the lower and higher outermost hardness at 2.68 and 4 m/s seemed to correspond to higher and lower wear losses, respectively.
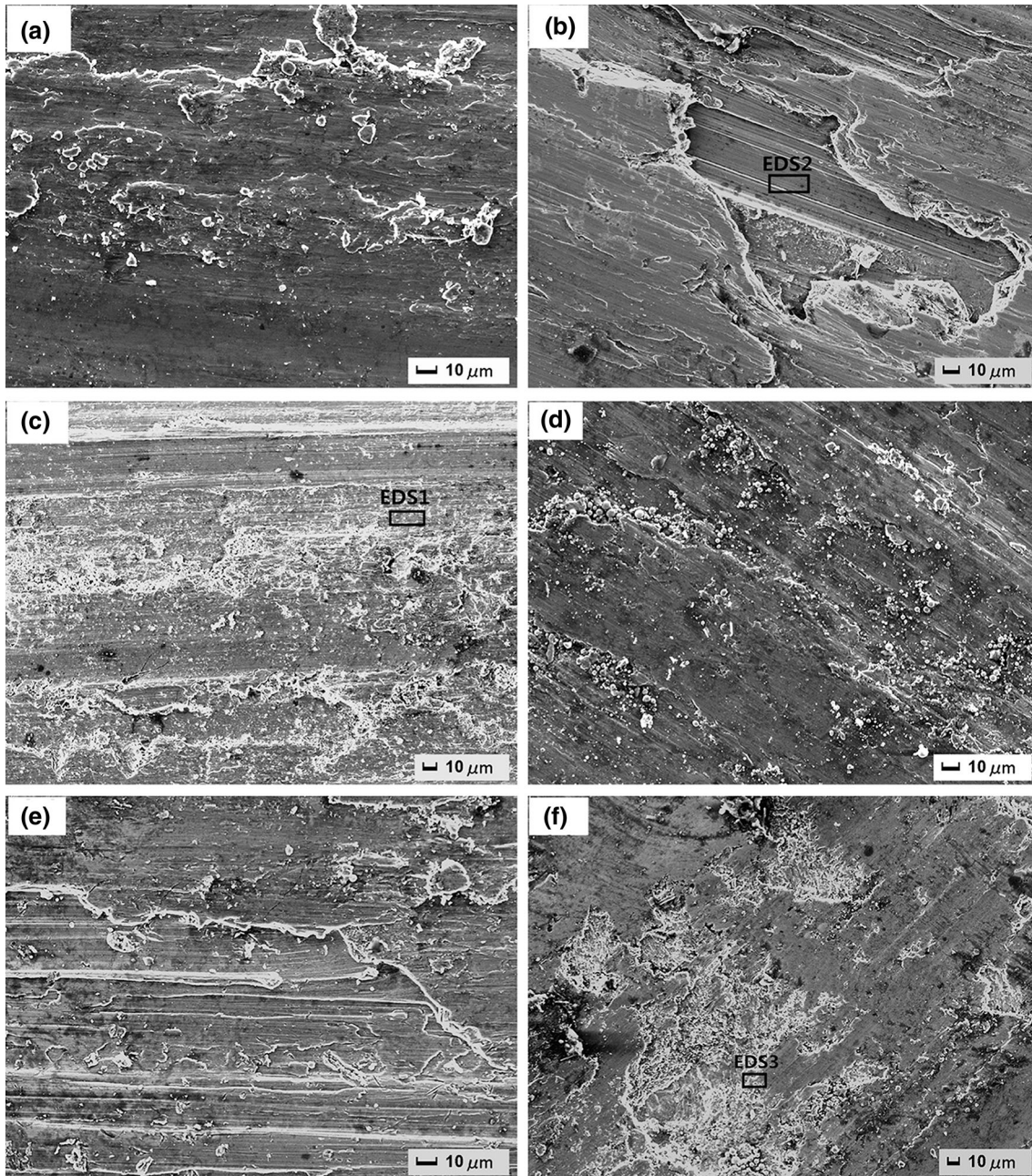
Fig. 3 Morphologies of worn surfaces of the aluminized Ti-6Al-4V at different sliding velocities (10 and 50 N, respectively): (a, b) 0.75 m/s; (c, d) 2.68 m/s; and (e, f) 4 m/s

4. Discussion

4.1 Formation of Tribo-Layers Under Various Sliding Speeds

The sliding wear of metal alloys was described by Rigney to be the evolution of the following phenomena: surface and subsurface plastic deformation, formation of debris and material transfer, reaction with the environment and mechanical mixing, and finally the formation of a mechanically mixed layer
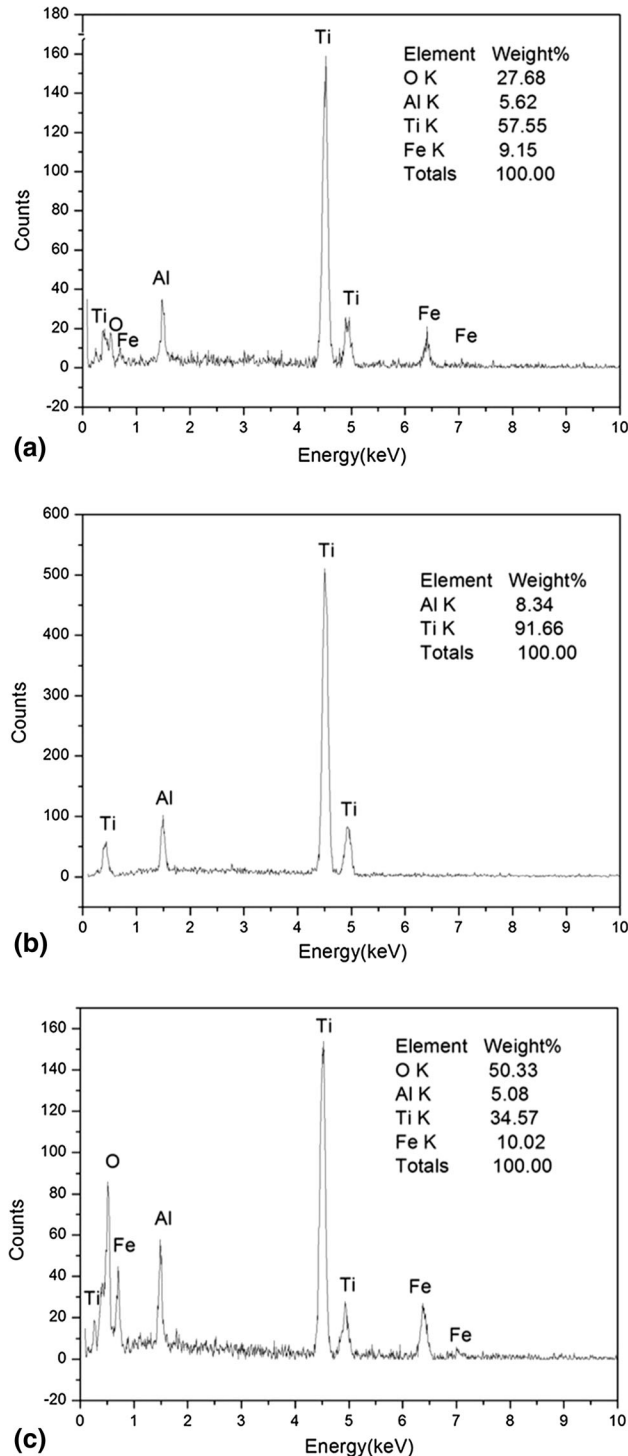

Fig. 4 EDS analysis of regional areas on worn surfaces in Fig. 4: (a) EDS$_1$, (b) EDS$_2$ and (c) EDS$_3$

(MML) on worn surfaces (Ref 26). As shown in the cross-sectional morphology of Fig. 6, tribo-layers were observed to from on worn surfaces. They were made of wear debris from the sliding pin and counterface metal by transfer as well as their reaction products with oxygen. Clearly, they were mechanically mixed layers (MML) from identifiable particles or compositions. Pauschitz et al. (Ref 27) classified the tribo-layers into three kinds: transfer layer, mechanically mixed layer (MML) and composite layer. They pointed out that mechanically mixed layer (MML) had an effect on reducing wear. However, whether the tribo-layers affected on wear behavior and mechanism or not, depended on the characteristics of tribo-layers. The characteristics of tribo-layers were decided by their formation processes under different sliding conditions (Ref 25).

The schematic diagram for the formation processes of tribo-layers is illustrated in Fig. 8. During dry sliding, the contact temperature of worn surfaces was raised due to more released friction heat with an increase in sliding velocity. On the one hand, the high contact temperature of worn surfaces resulted in the formation of oxides. On the other hand, the worn matrix would be softened. In addition, it must be noted that the produced wear debris would be partly retained to form tribo-layers and partly delaminated to cause wear loss. In other words, tribo-layers were made up with the residual wear debris. Under different sliding speeds, various wear debris were produced to form different tribo-layers. At 0.75 m/s, more small metal wear debris and less oxide wear debris were produced. In this case, tribo-layers would be made of more metal particles and a small quantity of oxide particles, as shown in Fig. 8(a). At 4 m/s, more oxide wear debris were produced because of more released heat. Thus, tribo-layers contained more oxides, as illustrated in Fig. 8(c). However, at 2.68 m/s, Fig. 8(b) shows that large-sized metal wear debris were produced and rapidly delaminated, Therefore, they were too difficult to be oxidized before delaminated. As demonstrated in Fig. 3(b), almost no oxide existed on worn surfaces, especially at 50 N. It can be deduced that merely metal-predominant tribo-layers were formed at 2.68 m/s.

4.2 Relations of Wear Resistance and Mechanism with Tribo-Layers, Coating and Matrix

Figure 9 illustrates the schematic diagram for the existing states of tribo-layer, the coating and the matrix during sliding. As shown in Fig. 9, the relations of wear resistance with the tribo-layer, the coating and the matrix were clarified through distinguishing their states in the acting area of friction force. At 0.5-2.68 m/s, metal-predominant tribo-layers formed on worn surfaces; the coating was totally consumed during sliding because of their weak protection. Tribo-layers and the matrix existed in the acting area of friction force and took effect. So the final state of the wear at 0.5-2.68 m/s was decided by metal-predominant tribo-layers and the matrix, as shown in Fig. 9(a). As the sliding speed reached 4 m/s, tribo-oxide layers formed on worn surfaces; the coating was retained during sliding because of their strong protection. In the acting area of friction force, there were tribo-layers and the coating. Thus, the final state of the wear at 4 m/s was decided by tribo-oxide layers and the coating, as shown in Fig. 9(b).

From the wear loss and XRD analysis of worn surfaces, it is noticed that aluminized Ti-6Al-4V alloy presented a lower wear loss than uncoated Ti-6Al-4V alloy and almost no TiAl$_3$ on worn surfaces at lower sliding velocities. This demonstrated
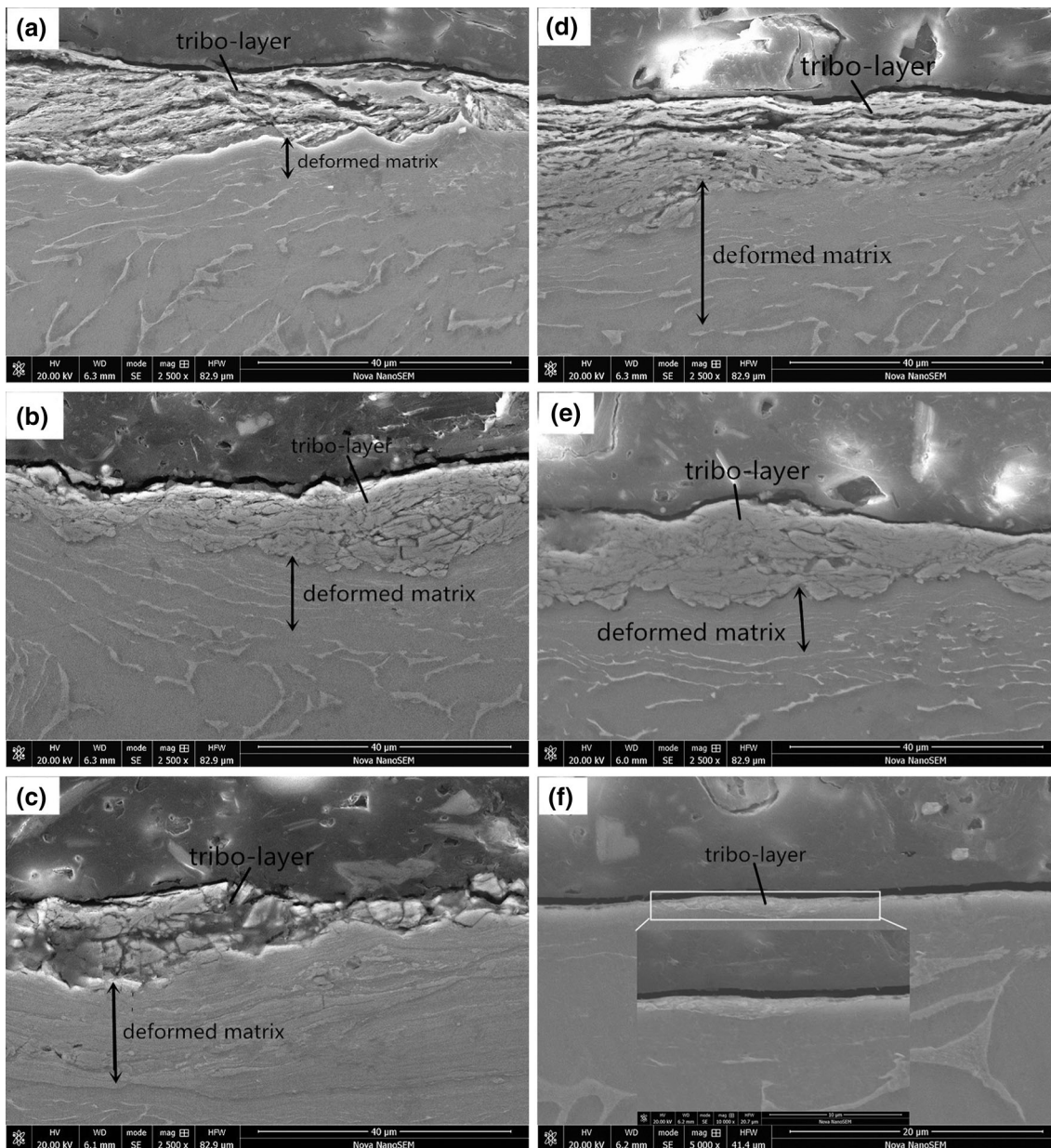
Fig. 5 Cross-sectional morphology of worn surfaces of the aluminized Ti-6Al-4V at different sliding velocities (10 and 50 N, respectively): (a, b) 0.75 m/s; (c, d) 2.68 m/s; and (e, f) 4 m/s

that aluminized Ti-6Al-4V alloy should possess a slight better wear resistance than untreated ones at lower velocities because of the function of $TiAl_3$ intermetallic compounds. However, at a high velocity, the $TiAl_3$ coating possessed a better wear resistance and still retained after wear, as shown in Fig. 6(a). Because of the brittleness of the $TiAl_3$ intermetallic compounds at room temperature, it was gradually consumed by brittle delamination during sliding, although the brittleness of the $TiAl_3$ intermetallic compounds would be slightly ameliorated with an increase in velocities. Thus, tribo-layers indeed played a key role in improving wear resistance of aluminized Ti-6Al-4V alloy, regardless of the existence and inexistence of the intermetallic coating. However, the existence of the intermetallic coating indeed provided a strong support for the protective tribo-oxide layer because of its high strength and thermal stability. Consequently, the intermetallic coating was helpful to
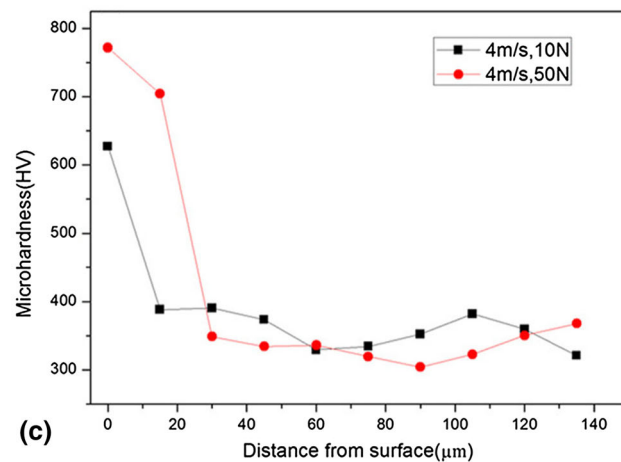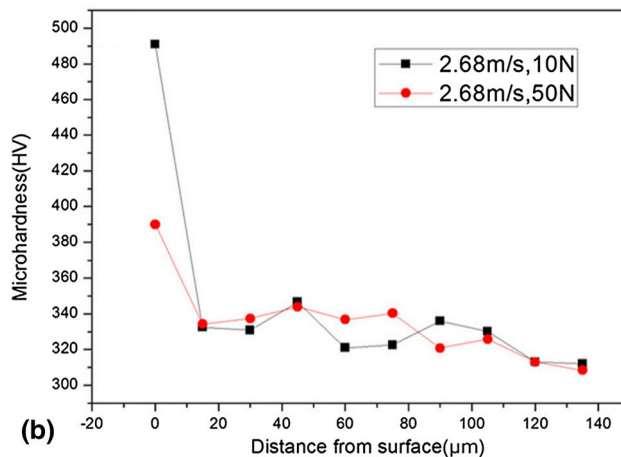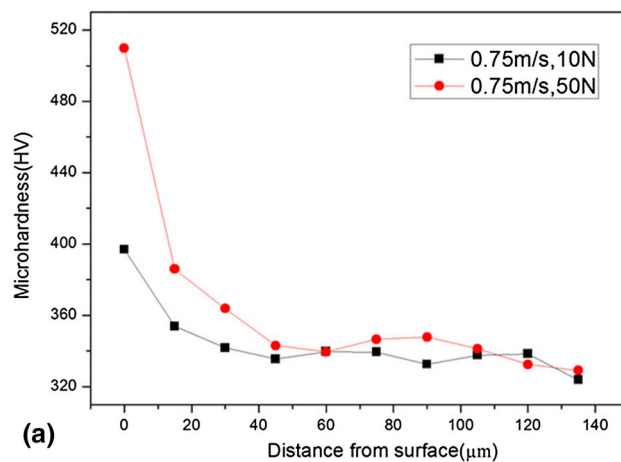
improve wear resistance of the titanium alloy. Conversely, compared with the intermetallic coating, the titanium alloy possessed relatively lower strength and thermal stability, presented a weak support for tribo-layers. As the matrix existed beneath the tribo-layers, they readily delaminated to result in high wear loss because of the deformation of the matrix.

Clearly, the tribo-layer became a key factor; its characteristics decided wear performance. The characteristics of tribo-layers are summarized in Table 1. Continuously increased velocity made tribo-layers contain more oxides and possess higher hardness, thus reducing wear loss obviously. It might be more important that trace Fe_2O_3 appearing at 4 m/s reduced the wear loss. In spite of trace amount, Fe_2O_3 would enhance the protective function of tribo-layers, which was reported to be a key factor to improve the elevated-temperature wear performance of titanium alloy (Ref 28,29). Moreover, with the
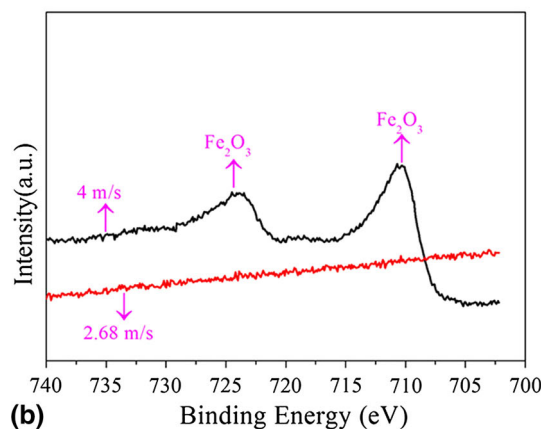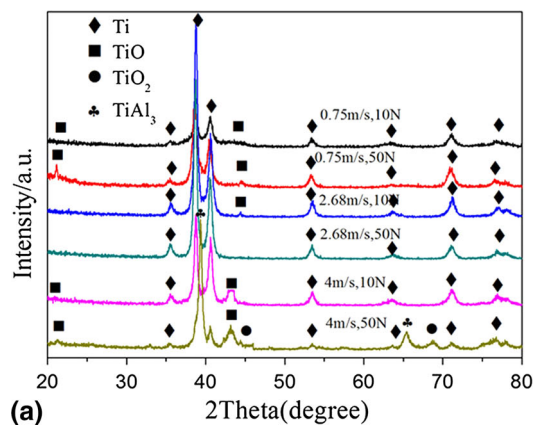
Fig. 6 XRD (a) and XPS spectra (b) of Fe 2p of worn surfaces of aluminized Ti-6Al-4V alloy sliding under various conditions

Fig. 7 Microhardness distribution of the cross-sectional worn surfaces of the aluminized Ti-6Al-4V at sliding velocities: (a) 0.75 m/s, (b) 2.68 m/s, and (c) 4 m/s

increase in sliding velocity, a higher temperature on the worn surface made tribo-layers to be readily compacted, from which their protective function would be benefited. However, on the other side, a higher temperature on the worn surface would cause the thermal softening of the worn matrix to present obvious plastic deformation of subsurface. Clearly, the softened matrix could not support the tribo-layers. Thus, they would be readily delaminated by the frictional force. This absolutely damaged the protective function of tribo-layers. In this case, under the action of pressure and frictional force, a lot of cracks appeared in tribo-layers, even they totally delaminated because tribo-oxide layers lost the solid support of substrate. At 0.75 m/s, the thickness of tribo-layers was about 10-20 μm, and the tribo-layers seemed to be uncompacted with cracks and a thick plastic deformed layer, especially about 5-10 μm at 50 N. At 2.68 m/s, tribo-layer became slightly thicker. The tribo-layers seemed to be uncompacted with a lot of cracks and a thicker plastic deformed layer (about 10-25 μm). On the contrary, at 4 m/s, the tribo-layer became thinner but very compact with a slight plastic deformed layer. Especially at 50 N, a plastic deformed layer could not be noticed. This meant that a total protection of tribo-layers was applied. The above-mentioned differences of tribo-layers at different velocities seemed to be closely related to the oxygen content and oxide amount. The oxygen content and oxide amount of the worn surfaces could be detected to be 28.71-29.88%O and trace TiO at 0.75 m/s, 13.01%O and a little TiO under 10 N, but zero and no oxide

under 50 N at 2.68 m/s, 37.27-45.33%O and TiO, TiO_2 and trace Fe_2O_3 at 4 m/s, respectively.

Oxygen content and oxide amount directly decided the characteristics and properties of tribo-layers. At 0.75 m/s, the existence of oxides endowed tribo-layers with ceramic-partly characteristics. Clearly, at 4 m/s, tribo-layers presented more obvious ceramic-dominated characteristics because of more oxides. Oppositely, at 2.68 m/s, tribo-layers merely presented metal characteristics because of no oxides. It is clear that the
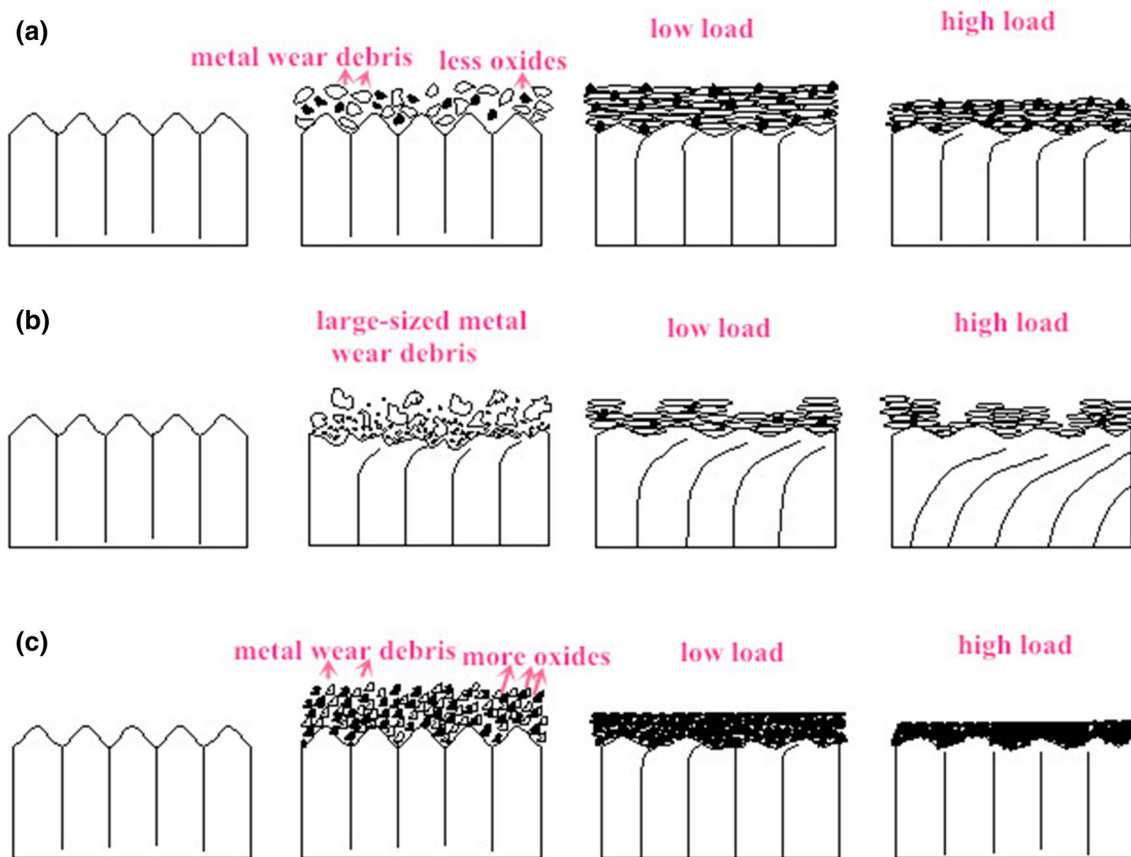
Fig. 8 Formation processes of tribo-layers at different sliding velocities (10 and 50 N, respectively): (a) 0.75 m/s; (b) 2.68 m/s; (c) 4 m/s
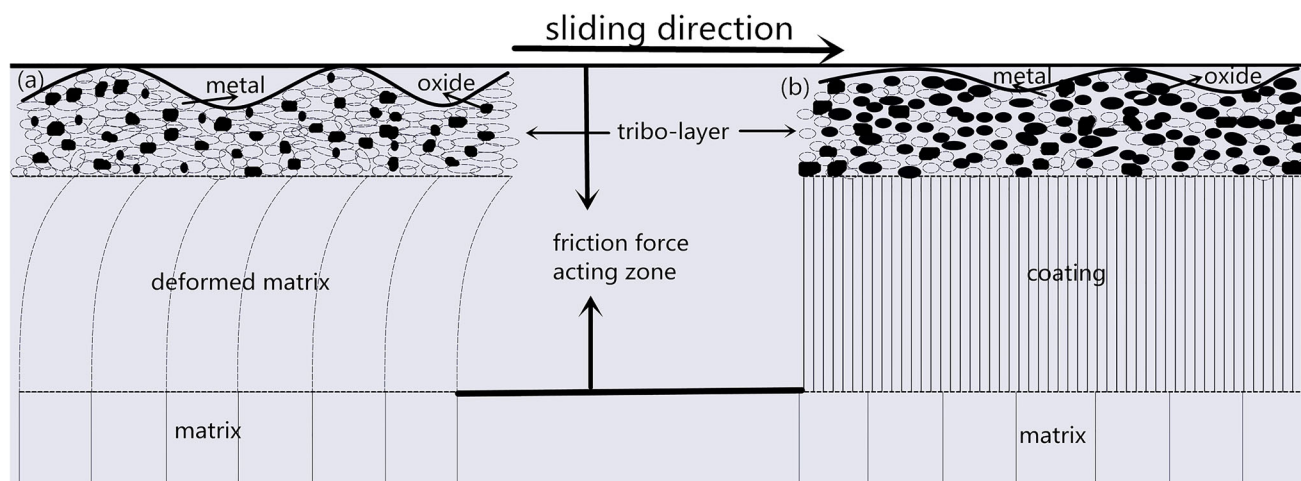
Fig. 9 Schematic diagram for the existing states of tribo-layers, the coating and the matrix during sliding

characteristics and properties of tribo-layers can be evaluated by microhardness. After sliding at various velocities, the tribo-layers presented much higher microhardness than the substrate, especially at 4 m/s; the hardness value reached 628-772 HV. However, at 2.68 m/s, the hardness of tribo-layer was substantially reduced because of the delamination of oxides, especially under 50 N. The protective function of tribo-layers can roughly be estimated through their hardness and variation as a function of load. At 0.75 m/s, the hardness of tribo-layers increased from 397 to 510 HV with the increase in load. Especially at

4 m/s, the hardness of tribo-layers increased from 628 to 772 HV with the increase in load. Clearly, tribo-layers became strong with the increase in load. Thus, such tribo-layers could be considered to be protective. Conversely, at 2.68 m/s, the hardness of tribo-layers decreased from 491 to 390 HV with the increase in load. Clearly, the latter approached the hardness (308-344 HV) of substrate. This demonstrated that tribo-layers became weak with the increase in load. And the tribo-layers presented similar characteristics and properties to the substrate alloy. So, such tribo-layers were suggested to be no protective.

Table 1 Characteristics of tribo-layers for aluminized Ti-6Al-4V alloy

Test condition	0.75, m/s		2.68, m/s		4, m/s	
Wear characteristics, N	10	50	10	50	10	50
Thickness (μm) of tribo-layer	15-20	10-20	10-15	10-20	10-20	8-10
Morphology of tribo-layer	Continuous, uncompacted	Continuous, compact	Continuous, uncompacted	Discontinuous, uncompacted	Continuous, compact	Continuous, compact
Thickness (μm) of a plastic deformed layer	1-5	5-10	10-15	10-25	1-5	0
Oxygen content (wt.%) of worn surface (EDS)	28.71	29.88	13.01	0	37.27	45.33
Phases of worn surface (XRD)	Ti,TiO	Ti,TiO	Ti,TiO	Ti	Ti,TiO	Ti, TiO, TiO_2, trace Fe_2O_3
Microhardness (HV) of tribo-layer	397	510	491	390	704	772
Microhardness (HV) of substrate	320-380	320-360	312-336	308-344	320-373	303-350

On the basis of identified phases and compositions on worn surfaces, the SEM analysis for the worn-surface morphology was used to readily distinguish wear mechanism. At 0.75 m/s, the worn surface presented a composite pattern containing adhesive and tribo-oxide traces. So, adhesive wear and oxidative wear cooperated. With an increase in sliding speed, the temperature of worn surface became higher because of more released friction heat. In these cases, more oxides would appear. However, at 2.68 m/s, almost no or trace oxides were noticed; the worn surface presented a large piece of delaminated regions and tearing traces, especially obviously at the load of 50 N. Thus, the wear mechanism should be a delamination wear. At 4 m/s, a lot of oxides of TiO and TiO_2 appeared; the worn surface presented compacted tribo-oxide layer region and some delaminated regions. Undoubtedly, the wear mechanism at 4 m/s was typical oxidative wear.

5. Conclusions

(1) The wear resistance of the titanium alloy was improved by the aluminized coating under various conditions, especially 4 m/s. The improved wear performance was suggested to be attributed to Ti-Al coating and tribo-oxide layer.

(2) $TiAl_3$ coating would be totally consumed because of its room-temperature brittleness and the weak protection of tribo-layers during wear at 0.5-2.68 m/s. At 4 m/s, $TiAl_3$ coating was retained because of its improved toughness and the strong protection of tribo-oxide layers.

(3) Tribo-layers were identified to form on worn surfaces under various conditions but their influence on the wear behavior and mechanism was decided by the amount and kind of oxides. The formation of tribo-layers under various sliding speeds was noticed to be a process including wear debris production, oxidation and accumulation and densification, even sintering.

(4) The outmost values of microhardness distribution at worn subsurfaces as a function of load could be used to identify their property and stability of tribo-layers. When the outmost hardness increased with an increase in load, tribo-layers were noticed to be strong, stable and protective. Conversely, the decreased hardness demonstrated a weak, instable and non-protective tribo-layer.

(5) At 4 m/s, oxide-containing tribo-layers with more TiO, TiO_2 and trace Fe_2O_3 presented high hardness and sta-bility, thus possessed an obvious wear-reduced function. Conversely at 2.68 m/s, no-oxide ones did not show the protection from wear because of their lower hardness and instability.

References

1. K. Phapale, S. Patil, S. Kekade, S. Jadhav, A. Powar, A. Supare, and R.K.P. Singh, Tool Wear Investigation in Dry and High Pressure Coolant Assisted Machining of Titanium Alloy Ti6Al4V with Variable α and β Volume Fraction, *Proc. Manuf.*, 2016, **6**, p 154–159
2. S. Bruschi, R. Bertolini, and A. Ghiotti, Coupling Machining and Heat Treatment to Enhance the Wear Behaviour of an Additive Manufactured Ti6Al4V Titanium Alloy, *Tribol. Int.*, 2017, **116**, p 58–68
3. D. Kumar, S.N. Akhtar, A.K. Patel, J. Ramkumar, and K. Balani, Tribological Performance of Laser Peened Ti–6Al–4V, *Wear*, 2015, **322**, p 203–217
4. I.L. Lebedeva and G.N. Presnyakova, Adhesion Wear Mechanisms Under Dry Friction of Titanium Alloys in Vacuum, *Wear*, 1991, **148**, p 203–210
5. A. Molinari, G. Straffelini, B. Tesi, and T. Bacci, Dry Sliding Wear Mechanisms of the Ti6Al4V Alloy, *Wear*, 1997, **208**, p 105–112
6. G. Straffelini and A. Molinari, Dry Sliding Wear of Ti-6Al-4V Alloy as Influenced by the Counterface and Sliding Conditions, *Wear*, 1999, **236**, p 328–338
7. Md Ohidul Alam and A.S.M.A. Haseeb, Response of Ti-6Al-4V and Ti-24Al-11Nb Alloys to Dry Sliding Wear Against Hardened Steel, *Tribol. Int.*, 2002, **35**, p 357–362
8. J. Qu, P.J. Blau, R.T. Watkins, O.B. Cavin, and N.S. Kulkarni, Friction and Wear of Titanium Alloys Sliding Against Metal, Polymer, and Ceramic Counterfaces, *Wear*, 2005, **258**, p 1348–1356
9. K.G. Budinski, Tribological Properties of Titanium Alloys, *Wear*, 1991, **151**, p 203–217
10. H. Dong and T. Bell, Enhanced Wear Resistance of Titanium Surfaces by a New Thermal Oxidation Treatment, *Wear*, 2000, **238**, p 131–137
11. N. Chelliah and S.V. Kailas, Synergy Between Tribo-Oxidation and Strain Rate Response on Governing the Dry Sliding Wear Behavior of Titanium, *Wear*, 2009, **266**, p 704–712
12. G. Straffelini, A. Andriani, B. Tesi, A. Molinari, and E. Galvanetto, Lubricated Rolling–Sliding Behaviour of Ion Nitrided and Untreated Ti-6Al-4V, *Wear*, 2004, **256**, p 346–352

13. C. Martini and L. Ceschini, A Comparative Study of the Tribological Behavior of PVD Coatings on the Ti-6Al-4V Alloy, *Tribol. Int.*, 2011, **44**, p 297–308

14. F. Borgioli, E. Galvanetto, F.P. Galliano, and T. Bacci, Sliding Wear Resistance of Reactive Plasma Sprayed Ti-TiN Coatings, *Wear*, 2006, **260**, p 832–837

15. Y.S. Tian and C.Z. Chen, Microstructures and Wear Properties of In Situ Formed Composite Coatings Produced by Laser Alloying Technique, *Mater. Lett.*, 2007, **61**, p 635–638

16. K. Sobiyi and E. Akinlabi, Microstructural Investigation of Ti Coating on Ti6All4V by Laser Cladding, *Mater. Today Proc.*, 2017, **4**, p 244–249

17. X. Li, L. Wang, X. Yu, Y.F. Feng, C.T. Wang, K. Yang, and D. Su, Tantalum Coating on Porous Ti6Al4V Scaffold Using Chemical Vapor Deposition and Preliminary Biological Evaluation, *Mater. Sci. Eng.*, 2013, **33C**, p 2987–2994

18. D. Nolan, S.W. Huang, V. Leskovsek, and S. Braun, Sliding Wear of Titanium Nitride Thin Films Deposited on Ti-6Al-4V Alloy by PVD and Plasma Nitriding Processes, *Sur. Coat. Technol.*, 2006, **200**, p 5698–5705

19. S. Djanarthany, J.-C. Viala, and J. Bouix, An overview of Monolithic Titanium Aluminides Based on Ti₃Al and TiAl, *Mater. Chem. Phys.*, 2001, **72**, p 301–319

20. D.V. Lazurenko, I.A. Bataev, I.S. Laptev, A.A. Ruktuev, I.N. Maliutina, M.G. Golkovsky, and A.A. Bataev, Formation of Ti-Al Intermetallics on a Surface of Titanium by Non-vacuum Electron Beam Treatment, *Mater. Character.*, 2017, **134**, p 202–212

21. S.Y. Lyu, Y.B. Sun, L. Ren, W.L. Xiao, and C.L. Ma, Simultaneously Achieving High Tensile Strength and Fracture Toughness of Ti/Ti-Al Multilayered Composites, *Intermetallics*, 2017, **90**, p 16–22

22. J.J. Dai, F.Y. Zhang, A.M. Wang, H.J. Yu, and C.Z. Chen, Microstructure and Properties of Ti-Al Coating and Ti-Al-Si System Coatings on Ti-6Al-4V Fabricated by Laser Surface Alloying, *Sur. Coat. Technol.*, 2017, **309**, p 805–813

23. H.S. Ren, H.P. Xiong, B. Chen, S.J. Pang, B.Q. Chen, and L. Ye, Microstructures and Mechanical Properties of Vacuum Brazed Ti₃Al/TiAl Joints Using Two Ti-Based Filler Metals, *Mater. Sci. Technol.*, 2016, **32**, p 372–380

24. T. Matsubara, T. Shibutani, K. Uenishi, and K.F. Kobayashi, Fabrication of a Thick Surface Layer of Al₃Ti on Ti Substrate by Reactive-Pulsed Electric Current Sintering, *Intermetallics*, 2000, **8**, p 815–822

25. X.X. Li, Y. Zhou, X.L. Ji, Y.X. Li, and S.Q. Wang, Effects of Sliding Velocity on Tribo-Oxides and Wear Behavior of Ti-6Al-4V Alloy, *Tribol. Int.*, 2015, **91**, p 228–234

26. D.A. Rigney, Transfer, Mixing and Associated Chemical and Mechanical Processes During the Sliding of Ductile Materials, *Wear*, 2000, **245**, p 1–9

27. A. Pauschitz, M. Roy, and F. Franek, Mechanisms of Sliding Wear of Metals and Alloys at Elevated Temperatures, *Tribol. Int.*, 2008, **41**, p 584–602

28. L. Wang, Q.Y. Zhang, X.X. Li, X.H. Cui, and S.Q. Wang, Severe-to-mild Wear Transition of Titanium Alloys as a Function of Temperature, *Tribol. Lett.*, 2014, **53**, p 511–520

29. L. Wang, Q.Y. Zhang, X.X. Li, X.H. Cui, and S.Q. Wang, Dry Sliding Wear Behavior of Ti-6.5Al-3.5Mo-1.5Zr-0.3Si Alloy, *Metall. Mater. Trans.*, 2014, **45**, p 2284–2296